Heat Powered Cycles
Conference 2023
Edinburgh
Heat in the new energy system

3rd to 6th of September 2023
The University of Edinburgh, Scotland

Analysis of two bed adsorption heat pump with a stratified storage to supply heating demands in a house for retrofitting of multi-family buildings

Alireza Sadeghlu[1*], Ferdinand Schmidt[1]

[1] Karlsruhe Institute of Technology (KIT), Institute of Applied Thermofluidics (IATF)

[*]Corresponding author: alireza.sadeghlu@kit.edu

Abstract

Gas driven heat pumps can contribute to a decarbonization of the building stock. A two-bed adsorption gas heat pump (TAGH) for multi-family buildings has been developed based on validated model. Due to the chosen sorption pair SAPO34/water, the heat pump can provide a temperature lift up to 42 °C, which is not sufficient for domestic hot water (DHW) preparation in stock buildings with circulation systems. Thus, the DHW preparation was achieved in a direct gas burner mode in order to prevent legionella contamination in the DHW circuit. This contribution analyses system aspects of hydraulic integration of a stratified heat storage and adapted controls for achieving two goals. First, a pre-heating of DHW in heat pump mode. Second, an increase in the seasonal system-level gas utilization efficiency (SGUE). In this regard, the analysis consists of three steps. First, the effect of system environment such as weather condition and design parameters have considered. Second, the hydraulic design, which includes the selection of extraction and insertion layers, plays its role in heat consumption and production. Finally, finding proper control strategy is a key factor in the analysis. To further increase of the SGUE, the system hydraulic configuration is redesigned with the help of second thermodynamic efficiency.

Keywords: Two bed adsorption heat pump, stratified storage, heating demands, control strategy, second thermodynamic efficiency, seasonal gas utilization efficienc

Introduction

The primary objective of the AdoSan project was to develop a two-bed adsorption gas heat pump (TAGHP) [1-3]. This was achieved through experimental validation and calibration of its individual components [4]. The specific focus of the project was to supply the heating demand in a space heating circuit, considering the guidelines mentioned in the VDI 4650-2 [5], with a nominal supply temperature of 55°C and a return temperature of 45°C [6]. The researchers sought to improve the gas utilization efficiency of the TAGHP at the system level by integrating various low temperature sources, including a borehole heat exchanger or building exhaust air [7]. The primary focus of the study was to assess the applicability of the two-bed adsorption gas heat pump (TAGHP) in a middle multi-family house (MMFH) [6] setting. In this context, a specialized storage unit called " hydraulic separator " was employed.

The study further evaluated the system's performance and achieved an annual gas utilization efficiency of 1.21 when utilizing a borehole heat exchanger. However, it is important to note that the TAGHP with a SAPO-34/water working pair in sorption mode has limitations in heating water beyond temperatures of 42°C. To fulfill higher temperature requirements, as specified in standards like VDI 4650-2 with 45/55°C [5], the heating process necessitates a "direct heating mode" where the gas burner directly supplies heat, bypassing the adsorption modules.

Given this context, the purpose of the investigation is to explore a system that addresses both water heating and space heating requirements by utilizing a two-bed adsorption gas heat pump (TAGHP). The main objective is to identify an integrated combi storage system and control scheme that enables the TAGHP to efficiently preheat domestic hot water (DHW), while simultaneously achieving gas savings in comparison to the reference configuration where DHW is consistently provided through direct heating mode.

System description

In the overall system configuration of the case study, two main components are considered. Firstly, there is the heat production component, which consists of TAGHPs utilizing both a high temperature source and a low temperature source, specifically a borehole heat exchanger. The TAGHP, composed of two modules, comprises one adsorber and one evaporator/condenser within a single casing. Its primary function is to generate heat. Secondly, there are two heat consumption components: a space heating circuit and a water heating circuit. These components make use of the heat generated by the TAGHP for their respective purposes.

In the case study configuration, there is also a combi-storage with 16 layers that acts as a central point of connection between the heat consumption and heat production components (see Figure1). This combi-storage is designed to store the excess heat and distribute it as needed.

To utilize the high-temperature source of TAGHP for heating the upper part of the combi-storage, a heat exchanger called HX_BRN_Stor is used. It links the combi-storage to the high-temperature source, transferring heat from BRN_HX_HT to the upper part of the tank. Moreover, HX_MTS connects TAGHP to the combi-storage, providing heat for the space heating circuit In Figure 1, it can be observed that the supply temperature is derived from layer 8 and is divided using a three-way valve. Approximately 0.1[kg/s] of the fluid is directed towards BR_HX_MT, while the remaining portion is directed towards HX_MTS. The return fluid from both HX_MTS and BR_HX_MT is then reintroduced into the combi-storage using an ideal inserter. This inserter ensures that the fluid is inserted into the nearest temperature layer within the tank, optimizing the heat distribution process. On the other hand, connecting the heat consumption parts to the combi-storage involves two steps. Firstly, there is a fresh water station (FWS) positioned between the user component and the combi-storage. The supply water is taken from the top layer of the combi-storage and directed to the FWS. The return fluid then flows back to the combi-storage with the help of an ideal inserter.

For the heat consumption component specific to a middle multi-family house (MMFH), it is connected to layer 6 of the combi-storage for the supply fluid and using an ideal inserter for return fluid to the combi-storage. This means that the heat produced by TAGHP and stored in the combi-storage is used to supply and circulate heat within the MMFH.

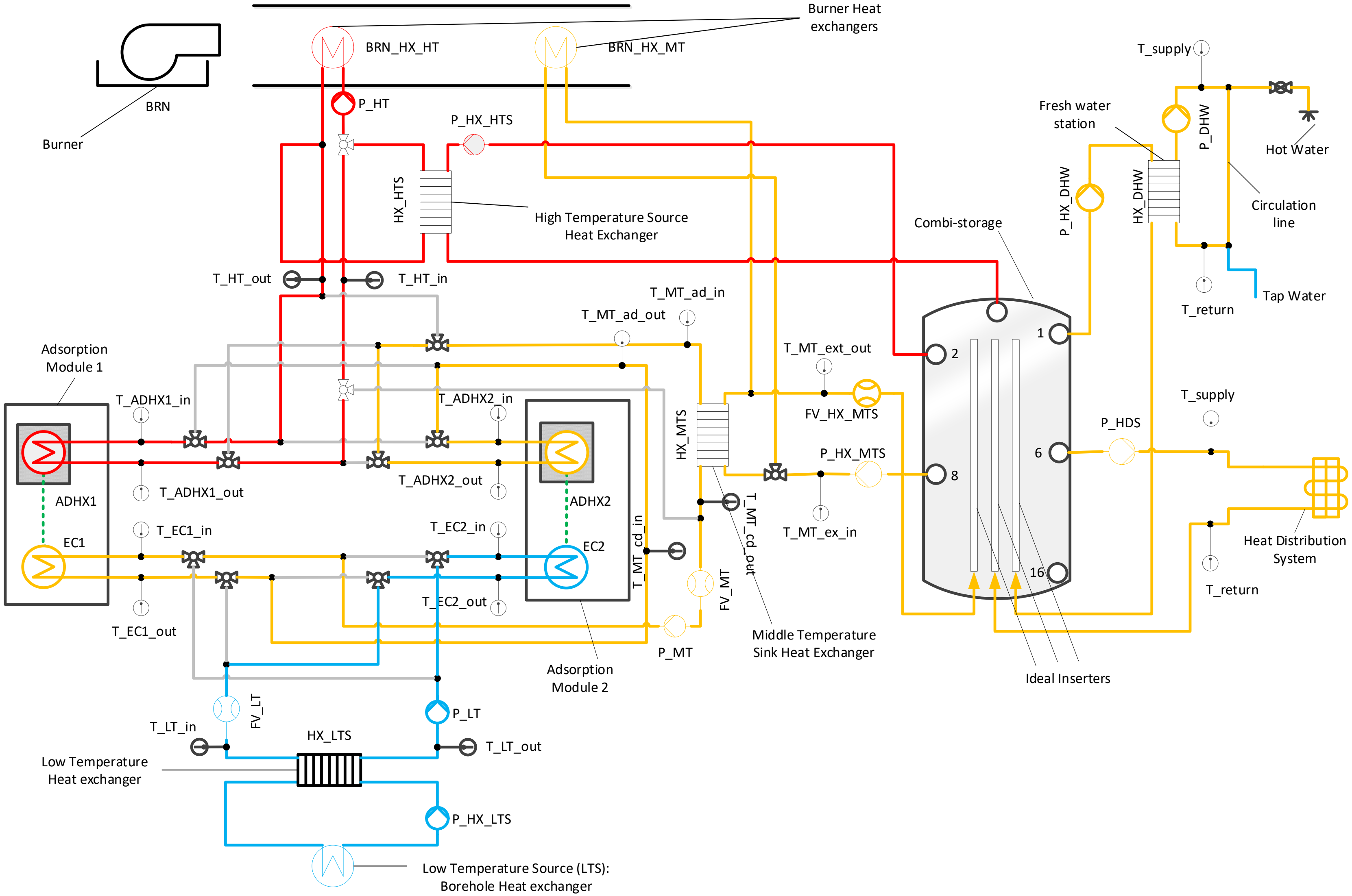

Figure 1: Schematic configuration in system level

Control Strategy

In this case study, there are three levels of control: component level, module level, and system level. At the component level, the mass flow rate of the pump for the user side of the Fresh Water Station (FWS) follows a loading profile every 10 minutes. The FWS serves a multi-family house (MMFH) with 12 apartments (4 with 1 occupant and 8 with 2 occupants). The mass flow rate on the user side of the system exhibits two distinct values. The first value corresponds to instances when tap water is being drawn off, and this value is determined based on the power profile for a multi-family household (MMFH). The second value is applicable when there is no demand for tap water, and in this case, the mass flow rate is set to 0.015 kg/s.

On the storage side, water is extracted from the top layer to create a temperature difference of 5°C in both sides of the heat exchanger. The mass flow rate of the pump in the storage side is controlled by a PI controller to maintain a user-side temperature of 60°C. The PI controller considers the user temperature as the measured value and the set point as 60°C. The output of the PI controller is multiplied by the maximum mass flow rate required for the user side. The return fluid from the FWS is directed to the combi-storage using an ideal inserter to store the lowest return temperature in the bottom part of the storage. In this case, the maximum temperature in the storage is 65°C, while the lowest temperature is around 16°C.

Moving to the other component control level, the space heating circuit is controlled by a PI controller that adjusts the mass flow rate of the supply water, extracted from layer 6, to maintain a room temperature of 20°C. The return water from the radiator is inserted back into the storage using another ideal inserter. For the heat production component, water is extracted from layer 2 and heated in HX_HTS, and then the return hot water is inserted into the top of the storage. Both pumps are controlled at the system level when the temperature of the top layer falls below 65°C.

At the module level, the control strategy of the heat pump (GHP) involves multiple processes such as adsorption, desorption, heat recovery, and direct heating mode. The GHP is activated based on two specific conditions. Firstly, the return temperature from the heating circuit should be below 34°C, considering the characteristics of the working pair SAPO-34/Water. Secondly, the evaporator inlet temperature needs to exceed 7°C. Once the outlet temperature in the adsorber reaches 90°C, the desorption process is ceased, and the heat recovery mode is initiated. During this mode, heat is transferred between the two modules to raise the temperature of the adsorption module while simultaneously cooling down the desorption module in preparation for the subsequent cycle. In the direct heating mode, the BRN_HX_HT is directly connected to the HX_MTS. This mode is activated when the power supplied to the space heating circuit falls below the power demanded. In such cases, the TAGHP exclusively focuses on heating up the storage using the high-temperature source until the supplied heat exceeds the heating demand. At the system level, the priority is to maintain a user temperature of 60°C. If the temperature in layer 1 falls below 63°C, the system prioritizes supplying the water heating circuit over the space heating circuit.

Discussion and Results

Figure 2 illustrates the RC (Resistor-Capacitor) diagram, providing a visual representation of the thermodynamic processes and heat transfer within the TAGHP system. In this diagram, each capacitor corresponds to the thermal mass of the materials, while each resistor represents the specific heat transfer mechanism, including conduction or convection. The diagram helps to understand the flow of energy and identify the various components involved. To further analyze the system's efficiency and identify areas of irreversibility, Table 1 provides a comprehensive list of factors and phenomena contributing to losses within each component of the TAGHP. This information enables a detailed assessment of the system's performance. In addition, a mathematical model has been implemented in Dymola to evaluate and quantify the system's overall efficiency and behavior. This modeling approach allows for in-depth analysis and optimization of the TAGHP system.

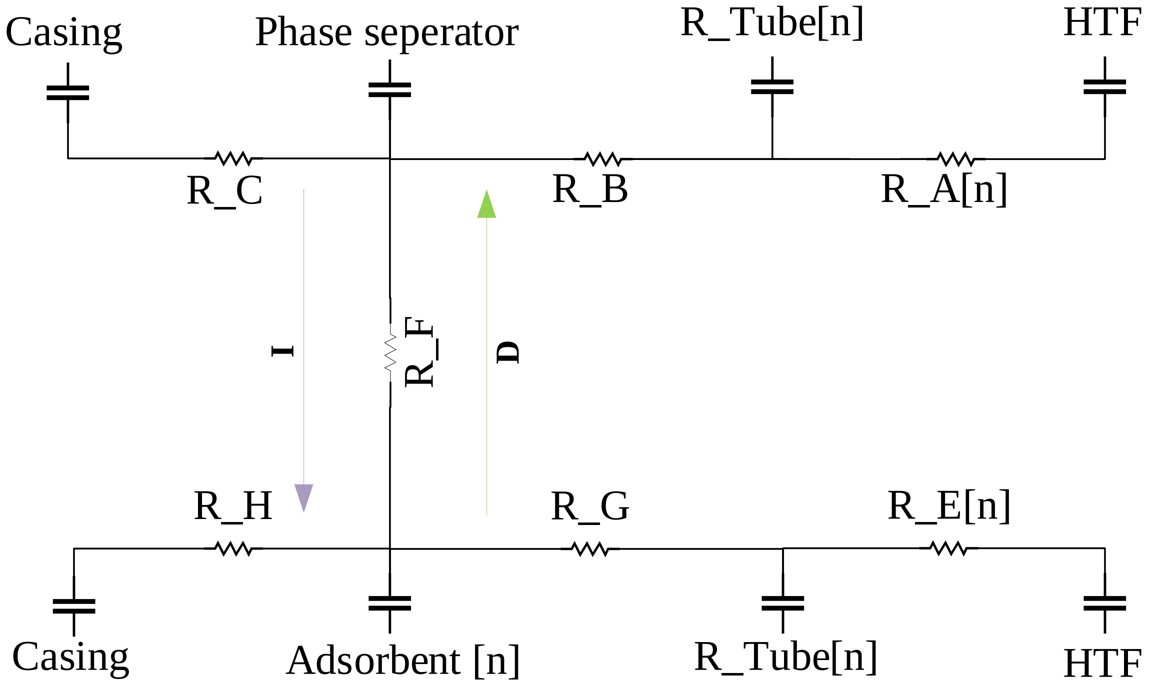

Figure 2. RC Diagram of the adsorber and Evaporator/Condenser

Table 1	
Ireversibility source originate from	
A	Mass and heat transfer between HTF and tube in Evaporator/Condenser
B	Heat transfer between Tube and Phase Separator
C	Heat transfer between Phase Separator and Casing
D	Desuperheat in Evaporator
E	Mass and heat transfer between HTF and tube in Adsorber
F	Heat transfer between Adsorber and Evaporator/Condenser
G	Heat transfer between working pair and Tube
H	Heat transfer between Tube and Casing
I	Superheat in Adsorber

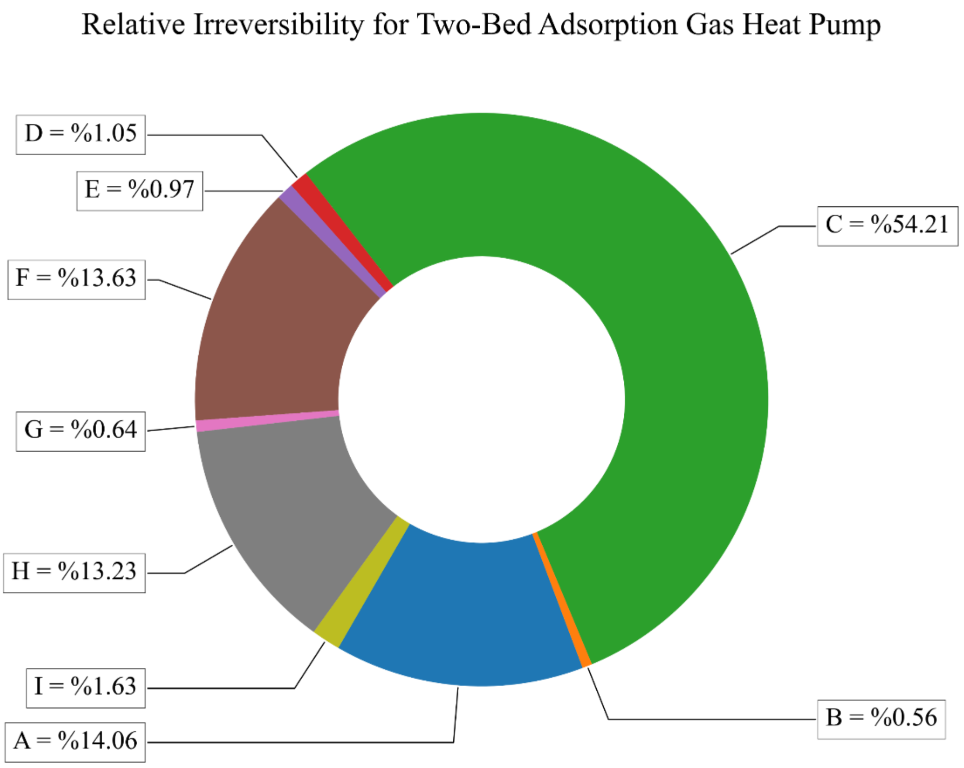

Figure 3: Ralative Irreversibility for various parts in Two-Bed Adsorption Gas Heat pump (TAGHP)

Figure 3 displays the annual relative irreversibilities for different parts of two bed adsorption gas heat pump.

It is clear that the largest source of irreversibility in the TAGHP system arises from the mass and heat transfer processes occurring between the Heat Transfer Fluid (HTF) and the tubes in the Adsorber. This particular aspect contributes significantly to the overall irreversibility within the system. Furthermore, the second-largest portion of relative irreversibility can be attributed to the presence of a finite temperature difference between the adsorber and the evaporator/condenser, as well as between the working pair and the tube. Additionally, the mass and heat transfer processes occurring between the HTF and the tubes, specifically within the evaporator and condenser heat exchanger pipes, play a significant role in comparison to other sources of irreversibility in the overall annual relative irreversibilities of the system.

$$RI = \frac{\dot{S}_{gen,i}}{\dot{S}_{gen,total,Module}} \tag{1}$$

$$\eta_{TAGHP} = \int_{0}^{365} \frac{p_{out}}{p_{in}} dt \tag{2}$$

$$\eta_{TAGHP} = \int_{0}^{365} \frac{p_{AGHP\_to\_stor\_for\_whc} + p_{AGHP\_to\_stor\_for\_shc}}{p_{in,ncv}} dt \tag{3}$$

$$\eta_{system} = \int_0^{365} \frac{p_{stor\_to\_whc} + p_{stor\_to\_shc}}{p_{in,ncv}} dt \tag{4}$$

$$\eta_{storage} = \int_0^{365} \frac{p_{stor\_to\_whc} + p_{stor\_to\_shc}}{p_{AGHP\_to\_stor\_for\_whc} + p_{AGHP\_to\_stor\_for\_shc}} dt \tag{5}$$

$$\dot{E}x_i = \dot{m} * (h_i - h_0 - T_0(s_i - s_0)) \tag{6}$$

$$\psi_{storage} = \frac{Ex_{output}}{Ex_{input}} = 1 - \frac{X_l + I}{Ex_{input}} \tag{7}$$

$$\psi_{storage} = 1 - \int_0^{365} \frac{\left(1 - \frac{T_0}{T_{ave,stor}}\right) p_{stor,loss} + T_0 \dot{S}_{gen}}{\dot{E}x_{AGHP\_to\_stor\_for\_whc} + \dot{E}x_{AGHP\_to\_stor\_for\_whc}} dt \tag{8}$$

Table 2	
$\dot{S}_{gen,i}$	Rate of Entropy generation in each component
$\dot{S}_{gen,total,Module}$	Sum of Entropy generation rates in condenser/evaporator and adsorber
$p_{AGHP\_to\_stor\_for\_whc}$	Power insert to the storage from HX_HTS to supply power for water heating circuit
$p_{AGHP\_to\_stor\_for\_shc}$	Power insert to the storage from HX_MTS to supply power for space heating circuit
$p_{stor\_to\_whc}$	Power insert to the water heating circuit from storage
$p_{stor\_to\_shc}$	Power insert to the space heating circuit from storage
$p_{in,ncv}$	Power source in net caloric value
$\dot{E}x_{AGHP\_to\_stor\_for\_whc}$	Rate of Exergy transfer by mass to the storage from HX_HTS to supply power for water heating circuit
$\dot{E}x_{AGHP\_to\_stor\_for\_whc}$	Rate of Exergy transfer by mass to the storage from HX_MTS to supply power for space heating circuit
X_l	Exergy loss through heat loss
I	Entropy loss through Heat and Mass transfer inside of the storage
$T_{ave,stor}$	Average storage temperature
$p_{stor,loss}$	Power loss from the storage

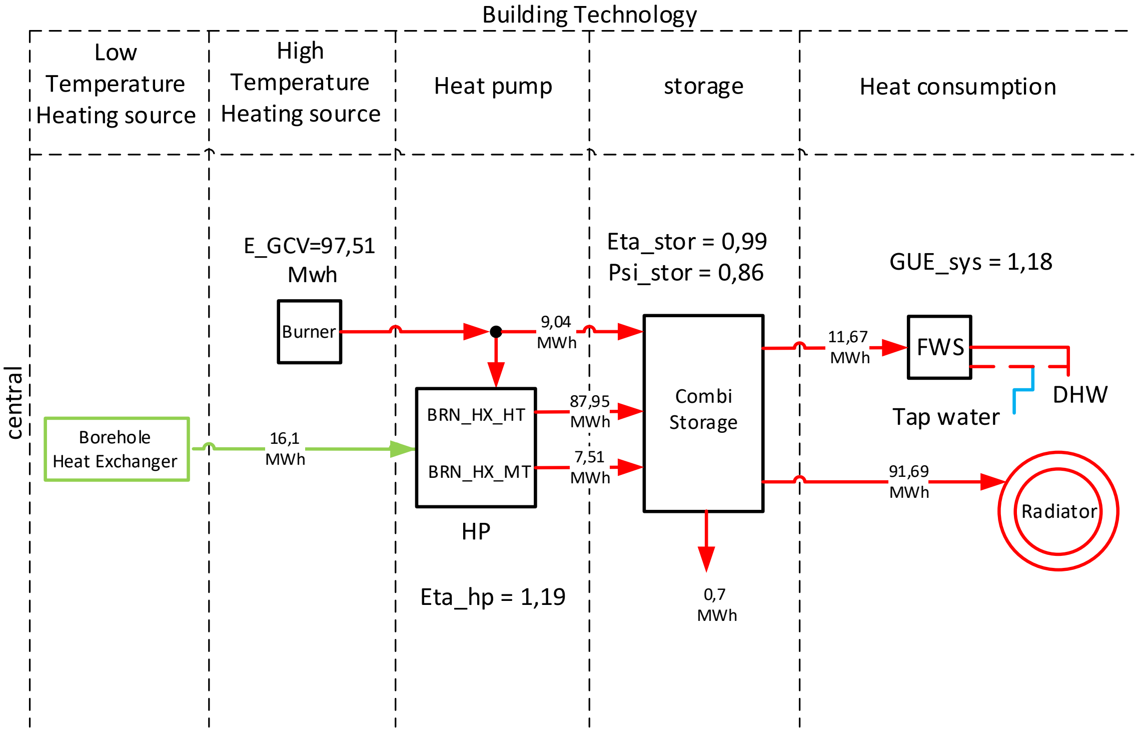

Figure 4: Annual energy flow in case study

The Annual Energy Flow diagram in Figure 4 provides a comprehensive overview of the energy production and consumption within the system. It clearly illustrates the energy generated by the Adsorption Gas Heat Pump (AGHP) and the burner, as well as the energy consumed by the various components. One of the primary objectives of this research is to pre-heat the water for the water heating circuit using the AGHP. Figure 4 highlights that the HX_HTS heat exchanger transfers 9.04 MWh of energy to the upper part of the storage tank, which is then utilized for the water heating circuit. However, the annual energy demand of the water heating circuit is 11.67 MWh, indicating a shortfall in energy supply. To bridge this gap, the AGHP steps in and supplies the remaining energy required for the water heating circuit.

The performance of both the system and the AGHP is assessed using two key parameters: the first law of thermodynamics and the second law of thermodynamics. The first law efficiency considers the net caloric value of the input gas power to determine the efficiencies of the system and the AGHP. On the other hand, the second law of thermodynamics considers the ratio of exergy output to exergy input, providing insights into the system's thermodynamic performance.

Additionally, to gain a more comprehensive understanding of the system's performance, the annual storage efficiencies have been calculated. These efficiencies, depicted in Figure 4 and Table 3, provide valuable insights into how effectively the system stores and distributes heat over the course of a year. By considering these storage efficiencies, a deeper understanding of the system's overall performance can be obtained.

Table 3

Efficiency	Value [-]
$\eta_{system,annual}$	1.18
$\eta_{TAGHP,annual}$	1.19
$\eta_{storage,annual}$	0.99
$\psi_{storage,annual}$	0.86

Figure 5 provides important temperature information for each layer, including the minimum, maximum, quartile, and median values. In this case study, the return fluid from each component is directed into the storage tank using an ideal inserter, except for the component that heats the upper part of the tank. The supply water for the high temperature source is obtained from layer 2, while the return temperature is directed to the top of the storage tank. Layer 1 represents the supply temperature for the Water Heating Circuit, whereas layer 6 corresponds to the supply temperature for the Space Heating Circuit. Layer 8 supplies the water for the GHP, enabling the utilization of the condenser and adsorption process heat. It's worth noting that the lowest temperature of the return fluid from the fresh water station determines the bottom temperature of the storage tank, and this temperature is also shown in figure 5.

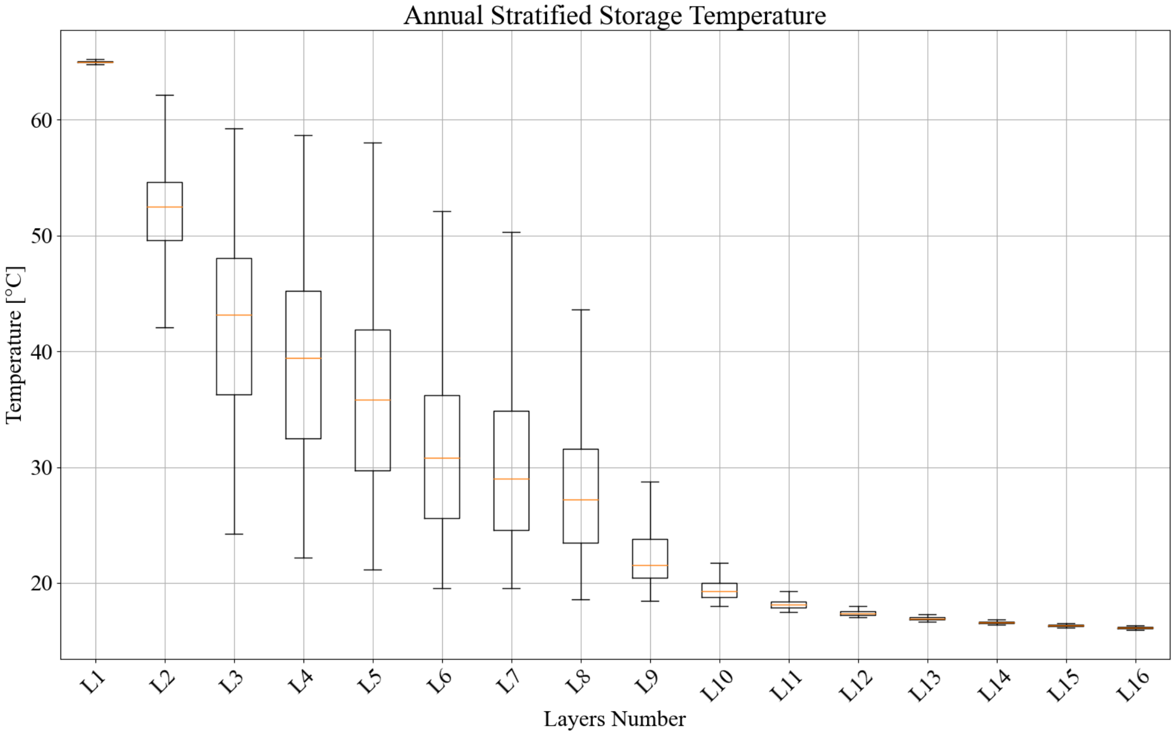

Figure 5: Annual storage temperature in different layers.

To prevent Legionella contamination in the water heating circuit, the system incorporates circulation to maintain a temperature of 55°C for the water inside the pipes when there is no water consumption. As a result, as shown in figure 6, the annual water temperature on the user side of the fresh water station (FWS) is consistently around 60°C. This measure helps ensure the water remains at a temperature that discourages the growth of Legionella bacteria.

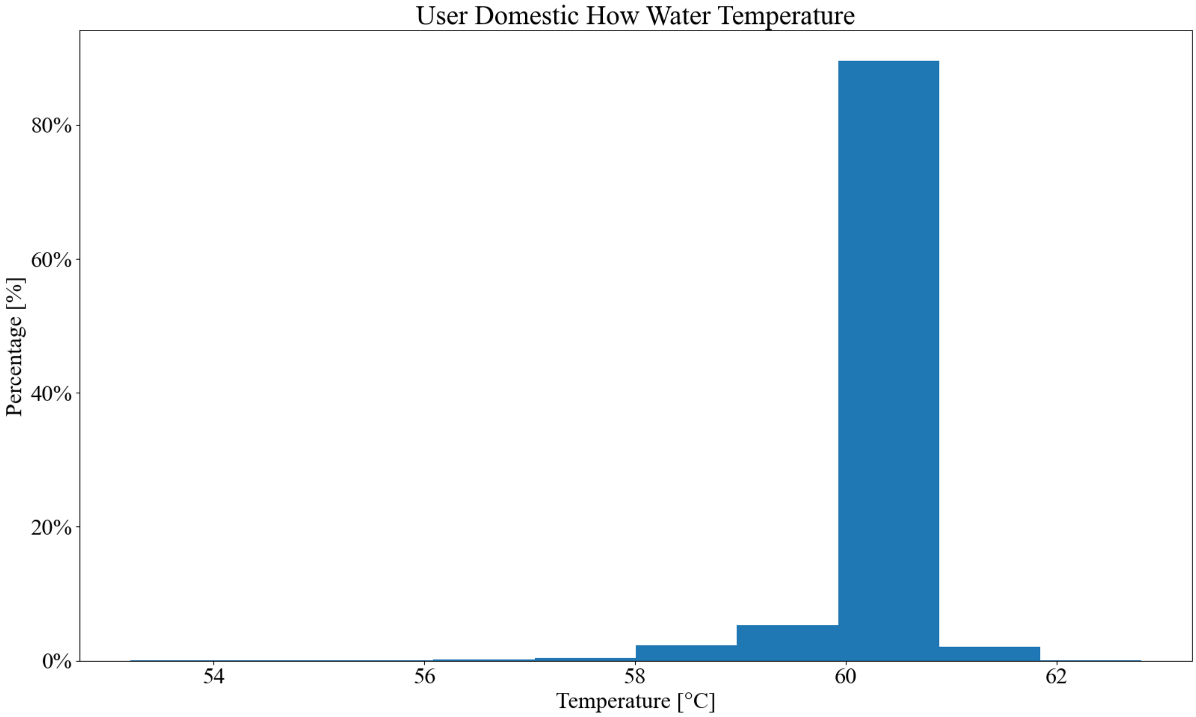

Figure 6: Supply temperature to the user in water heating circuit

Figure 7 presents the correlation between room temperature and outside temperature throughout the span of one year in Potsdam. The graph depicts this relationship by using lighter colors to indicate instances when the room temperature remains relatively stable at around 20°C, particularly during the cold season when the outside temperature drops below 15°C. It is worth noting that the annual simulation of the case study does not consider the presence of air conditioning. Therefore, as the outside temperature rises, the room temperature also experiences a corresponding increase.

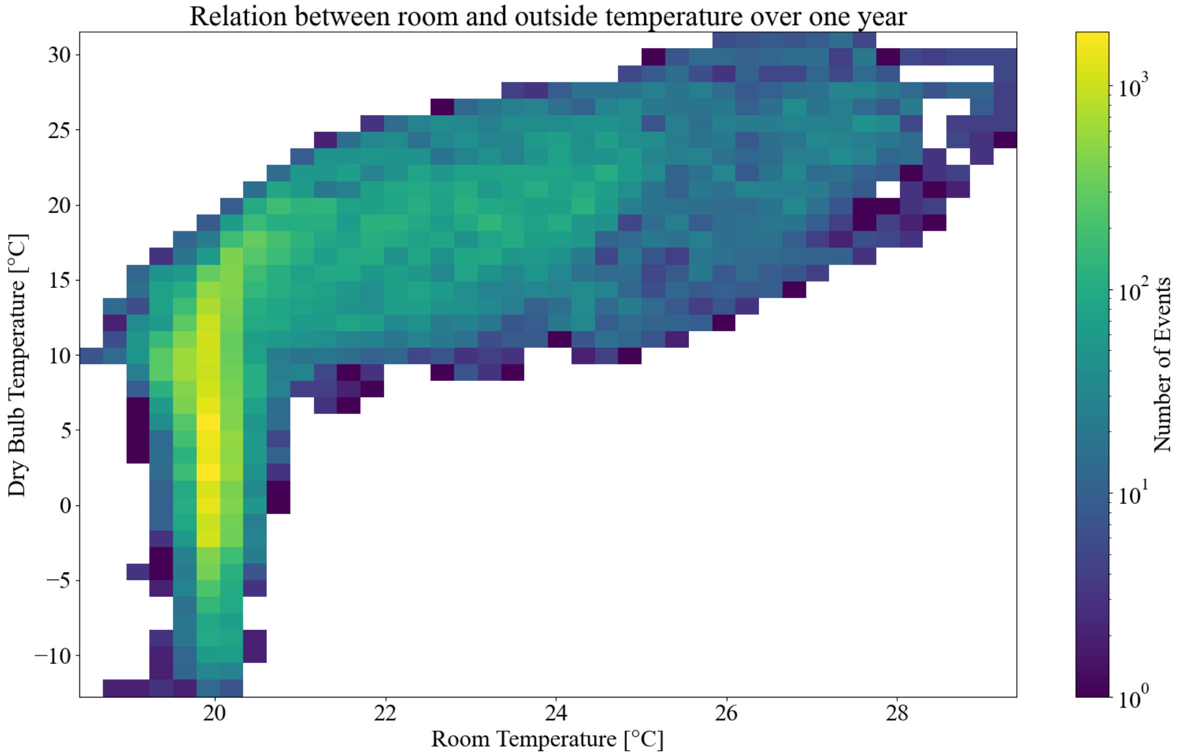

Figure 7: Change of room temperature with respect to the outside temperature over one year

Acknowledgements

I would like to express my sincere gratitude to the German Academic Exchange Service (DAAD) for providing financial support throughout my Ph.D. studies. Their generous funding has played a crucial role in enabling the successful completion of my research. I am truly grateful for their support and the opportunities they have provided me.

References

[1] Wittstadt, U., Füldner, G., Laurenz, E., Warlo, A., Große, A., Herrmann, R., Schnabel, L., Mittelbach, W., “A novel adsorption module with fiber heat exchangers: Performance analysis based on driving temperature differences”, Renewable Energy, 2017.

[2] Freni, A., Bonaccorsi, L., Calabrese, L., Caprì, A., Frazzica, A., Sapienza, A., “SAPO-34 coated adsorbent heat exchanger for adsorption chillers”, Applied Thermal Engineering, 2015.

[3] Bendix, P., Füldner, G., Möllers, M., Kummer, H., Schnabel, L., Henninger, S., Henning, H. M., “Optimization of power density and metal-to-adsorbent weight ratio in coated adsorbers for adsorptive heat transformation applications”, Applied Thermal Engineering, 2017.

[4] Riffel, D. B., Wittstadt, U., Schmidt, F. P., Núñez, T., Belo, F. A., Leite, A. P. F., Ziegler, F., “Transient modeling of an adsorber using finned-tube heat exchanger”, International Journal of Heat and Mass Transfer, 2010.

[5] *Kurzverfahren zur Berechnung der Jahresheizzahl und des Jahresnutzungsgrads von Sorptionswärmepumpenanlagen Gas-Wärmepumpen zur Raumheizung und*

Warmwasserbereitung, VDI 4650 Blatt 2, Verein Deutscher Ingenieure, Jan., 2013.

[6] Andersen, O., Dörr, H., Füldner, G., Groddeck, P., Herrmann, R., Herrmann, S., Kostmann, C., Sadeghlu, A., Schmalzried, H., Schmidt, F., Velte, A., Volmer, R., Wittstadt, U., *LowEx-Konzepte für die Wärmeversorgung von Mehrfamilien-Bestandsgebäuden; Entwicklung einer GasAdsorptionswärmepumpe für die Bestandssanierung: gemeinsamer Abschlussbericht AdoSan-LXB: Berichtszeitraum: 01.08.2018-28.02.2022 (FKZ 03ET1554A, B, C, E und F), 01.08.218-30.06.2022 (FKZ 03ET1554D)*, *[Online], Available*: **https://www.tib.eu/de/suchen/id/TIBKAT%3A182328843X**.

[7] Velte, A., Laurenz, E., Leisner, S., Weber. J., Wittstadt, U., Füldner, G., “Experimental Results of a Gas Fired Adsorption Heat Pump and Simulative Prediction of Annual Performance in a Multi-Family House”, Applied Thermal Engineering, 2022.